Cellular Physiology and Biochemistry

© 2018 The Author(s)
Published by S. Karger AG, Basel
www.karger.com/cpb

Open access

1188

Original Paper

The Sphingosine-1-Phosphate/ Sphingosine-1-Phosphate Receptor 2 Axis in Intestinal Epithelial Cells Regulates Intestinal Barrier Function During Intestinal Epithelial Cells–CD4+T-Cell Interactions

Tanzhou Chen   Ruoyang Lin   Sisi Jin   Renpin Chen   Haibo Xue   Huajun Ye   Zhiming Huang

Department of Gastroenterology and Hepatology, The First Affiliated Hospital of Wenzhou Medical University, Wenzhou, China

Abstract
Background/Aims: Epithelial cells line the intestinal mucosa and form an important barrier for maintaining host health. This study aimed to explore the mechanism of the Sphingosine-1-phosphate (S1P)/Sphingosine-1-phosphate receptor 2 (S1PR2) pathway in intestinal epithelial cells (IECs) that participate in the intestinal barrier function. *Methods:* In this study, we constructed a knockout of the S1PR2 gene in mice, and Dextra sulfate sodium (DSS) was used to induce colitis. We isolated IECs from wild type (WT) and S1PR2$^{-/-}$ mice, and the endogenous expression of S1PR2 and Zonula occludens 1 (ZO-1) in IEC were detected by Western blot. Next, the major histocompatibility complex II (MHC-II) expression was analyzed by reverse transcription quantitative real-time (RT-qPCR) and flow cytometry. The *in vivo* and *in vitro* intestinal permeability were evaluated by serum fluorescein isothiocyanate (FITC) concentration. The tumor necrosis factor-α (TNF-α), interleukin-6 (IL-6) and interferon-γ (IFN-γ) levels in cell suspension were analyzed by enzyme-linked immuno sorbent assay (ELISA). A carboxyfluorescein diacetate succinimidyl ester (CFSE) assay was used to detect the T-cell proliferation in a co-culture system. *Results:* The intestinal mucosal barrier damage in S1PR2$^{-/-}$ mice was more severe than in the WT mice, and there were more CD4+T-cells in the colon tissue of DSS-treated S1PR2$^{-/-}$ mice. Either the mouse colon carcinoma cell line (CT26. WT) or the IECs upregulated MHC-II expression, which then promoted CD4+T-cell proliferation. The S1P/S1PR2 pathway controlled MHC-II expression to regulate CD4+T-cell proliferation via the extracellular signal-regulated kinase (ERK) pathway. In addition, the IFN-γ that was

Tanzhou Chen and Zhiming Huang.

Dept. of Gastroenterology and Hepatology, The First Affiliated Hospital of Wenzhou
Med. University Nanbaixiang, Ouhai District, Wenzhou 325000, Zhejiang (China)
E-Mail cctzz@163.com, cctzz2008@126.com

KARGER

secreted by CD4+T-cells increased DSS-induced damage of intestinal epithelial cell barrier function. ZO-1 expression was increased by S1P in CT26.WT cells, while S1PR2 antagonist JTE-013 expression was downregulated. However, in CT26.WT$^{si-S1PR2}$ cells, S1P had no effect on ZO-1 expression. ***Conclusions:*** The S1P/S1PR2 axis in IECs mediated CD4+T-cell activation via the ERK pathway and MHC-II expression to regulate intestinal barrier function.

Introduction

Intestinal epithelial cells (IECs) maintain gastrointestinal homeostasis by providing a physical and functional barrier between the intestinal lumen and underlying mucosal immune system. S1P is a potent bioactive lipid mediator that has been shown to promote the proliferation of IECs and plays a pivotal role in enhancing barrier function in intestinal tissues [1, 2]. Five cognate G protein-coupled receptors (S1P(1–5)) have been shown to mediate various cellular effects of S1P, and S1PR2 has recently been implicated in the regulation of the pro-adhesion and pro-inflammatory phenotype of the endothelium [3]. Our previous study [4] found that S1P-mediated activation of S1PR2 plays an important role in regulating IEC proliferation and migration. In addition, S1PR2 activated by S1P had a protective effect on the integrity and permeability of the intestinal mucosal barrier via a PI3K/Akt dependent mechanism [5]. However, the mechanism of the S1P/S1PR2 pathway in IEC participation in the intestinal barrier function is not entirely clear.

Normal IECs could be used as APCs to activate CD4+T-cells. Previous studies have reported that co-cultures of normal T cells and IECs derived from inflammatory bowel disease (IBD) patients result in the preferential activation of CD4+T-cell proliferation and IFN-γ secretion, suggesting the IBD IECs contributed to the CD4+T-cell activation that was associated with significant IFN-γ [6]. Moreover, the S1P/S1PR2 axis was found to regulate early airway T-cell infiltration in murine mast cell dependent acute allergic responses [7]. Therefore, the aim of this study was to determine the mechanism of the S1P/S1PR2 axis in IEC participation in the intestinal barrier function that was associated with CD4+T-cell activation.

In this study, we constructed S1PR2$^{-/-}$ mice, which were then treated with dextran sulfate sodium (DSS) to induce colitis. After treatment, colonic IECs were isolated and taken from DSS-induced S1PR2$^{-/-}$ mice to be used as a co-culture with normal CD4+T-cells. In addition, a purchased mouse colon carcinoma cell line that was transfected by a lentivirus of RNA interference for gene S1PR2 (CT26.WT$^{si-S1PR2}$ cells) was treated with DSS/IFN-γ and then co-cultured with CD4+T-cells. Our results suggest that the S1P/S1PR2 axis in IECs mediated CD4+T-cell activation via the ERK pathway and also mediated MHC-II expression to regulate intestinal barrier function.

Materials and Methods

Animal model and detection

Male and female C57BJ6 mice aged 8–12 weeks were used in the experiment. They were housed in temperature- and humidity-controlled rooms kept on a 12 h light/dark cycle and provided unrestricted amounts of food and water; the bedding was changed twice a week. Knockout of the S1PR2 gene in the mice was performed as previously described [8, 9]. Dextra sulfate sodium (DSS, molecular weight 36000-50000) was dissolved in the drinking water provided to the mice, and a fresh DSS solution was provided every day. WT and S1PR2$^{-/-}$ mice (n = 5) were exposed to 2.0% DSS for 7 d to induce colitis. Then they were provided normal water for 7 d and killed at 14 d [10]. Changes in the mice's body weight and deaths were observed daily. After dissecting the mice, the total length of the mouse colon was measured. The mice used in the present study were treated according to the protocols approved by the ethical committee of the First Affiliated Hospital of Wenzhou Medical University.

KARGER

Cellular Physiology and Biochemistry

Cell Physiol Biochem 2018;48:1188-1200

DOI: 10.1159/000491985
Published online: July 25, 2018

© 2018 The Author(s). Published by S. Karger AG, Basel
www.karger.com/cpb

1190

Chen et al.: S1P/S1PR2 Pathway in the Intestinal Barrier Function

Detection of intestinal permeability in mice

Fluorescein isothiocyanate-dextran (FITC-dextran) (Sigma-Aldrich, St. Louis, MO, USA) was used to analyze intestinal permeability *in vivo* as described previously [10]. Standard curves were obtained by diluting the FITC-dextran in non-treated plasma diluted with PBS (1:3 v/v). Briefly, mice fasted for 6 h before being given a 50 mg/ml FITC-dextran gavage (0.6 mg/g body weight). After 1 h, 120 ul of blood was collected from the tip of the caudal vein prior to DSS treatment. After dosing the mice with DSS, FITC-dextran was given at the end of the experiment or upon death, and 120 ul of blood was collected via cardiac puncture. The collected blood was centrifuged, and the plasma was diluted in PBS (1:1 v/v, pH 7.4). The FITC-dextran concentration was then analyzed using a Synergy HT multi-mode microplate reader (BioTek, Winooski, VT, USA) at 485 nm excitation wavelength and 535 nm emission wavelength.

Paracellular permeability measurement

After an intestinal epithelial barrier model was successfully constructed, LPS was added in the apical side of the model and cultured with a supplementary 1 mg/mL FD-4 solution for 2 h. The paracellular permeability was then measured using FD-4 flux. A Synergy H2 microplate reader (BioTek, Winooski, VT, USA) was used for the determination of FD-4 signaling.

Western blot analysis

Using lysis in a RIPA buffer and centrifugation for 20 min, proteins were extracted from the tissue or cells, and the Bradford method was used to detect the quality of the proteins. SDS-PAGE was used to separate the proteins in equal amounts, and the proteins were then transferred onto PVDF membrane with primary antibodies (Sigma-Aldrich, St. Louis, MO, USA) against S1P, S1PR2, ZO-1, occluding and p-ERK at 4°C for 24 h. Then, the membrane was incubated with secondary antibodies at room temperature for another 1 h. β-actin was used as the internal control.

Preparation of cell suspension of colonic tissue

The mice were killed by cervical dislocation, placed in a supine position, and the skin and abdominal peritoneum were cut to open the abdominal cavity. The whole colon was cut to measure the length, and then the intestinal contents were removed and the intestines cleaned with Hank's free balanced salt solution containing 1% FBS and free of calcium and magnesium (CMF-HBSS). The intestines were cut into 2 mm portions, soaked in CMF-HBSS containing 3 mM EDTA and placed on the desktop thermostatic oscillator at 180 rpm/min for 30 min at 37°C. After centrifugation, the precipitate was digested for 1.5 h with HBSS that contained 1 mg/mL IV collagenase and DNA enzyme I. After removing the impurities and undigested tissue blocks with a 300 mesh screen, we obtained the cell suspension of the mouse colon tissue.

ELISA assay

The obtained mice colon cell suspension was centrifuged and cleaned by PBS two times, and then the cells were resuspended in an RPMI 1640 medium containing 10% FBS. After counting, the cells were seeded in 24-well plates ($4*10^5$ cells) for 24 h. Supernatants were assayed for TNF-α, IL-6 and IFN-γ with an ELISA kit (R&D Systems, Minneapolis, MN, USA).

Flow cytometric analysis

The obtained mouse colon cell suspension was centrifuged, cleaned and resuspended in 1 ml PBS containing 20 μl BSA (10%) and then incubated for 30 min at 4°C. After 30 min, the cells were washed in PBS two times, and then 20 μl CD4-PE was added to the tube, and the suspension was placed in a dark location for another 30 min. The cells were washed in PBS two times, and 500 μl PAF (4%) was added to the tube. After 30 min culturing and centrifugation, 50 μl Trixon-100 (0.1%) was added to the tube for 10 min. After centrifugation, the supernatant was discarded, and the cells were resuspended in 100 μl PBS. After adding 2 μl IFN-γ-FITC, the cells were incubated at 4°C for 30 min in a dark location. Finally, the CD4$^+$T-cells and CD4$^+$ IFN-γ$^+$ T cells were analyzed with a flow cytometer (Beckman Coulter, Fullerton, CA, USA).

Colon histology

The middle section of the colon was fixed in 10% formalin before hematoxylin and eosin (H&E) staining. Light microscopy (Olympus IX70, Olympus, Shinjuku, Tokyo, Japan) was used to observe the colon histology.

Isolation of colonic IECs and CD4+T-cells

Primary murine colonic epithelial cells were isolated from 4- to 6-week-old C57BL/6 mice. Briefly, the colon was opened longitudinally to expose the mucosal surface and then washed with HBSS free of calcium and magnesium and supplemented with gentamicin (100 mg/ml), Fungizone (100 mg/ml), penicillin (100 U/ml) and streptomycin (100 mg/ml). Five-millimeter segments of tissue were then incubated for 90 min at 37°C in a 10 ml DMEM culture medium that contained 20% Nu-Serum (Collaborative Biomedical Products Becton Dickinson, Franklin Lakes, NJ, USA), 2% Luria broth, 4 mM L-glutamine, 50 mg/ml gentamicin, 50 U/ml penicillin, 50 mg/ml streptomycin and 0.4% Bactrim along with 10 mg Dispase I (Boehringer Mannheim Biochemicals, Mannheim, Germany) in a 50 ml centrifuge tube with constant gentle rotation. The digest was then passed through a steel mesh sieve to remove mucus and undigested fragments of tissue. The recovered cells were washed twice in HBSS, and the cell pellet was analyzed directly or placed into culture. The purity of each epithelial cell preparation was evaluated by cytokeratin staining and by determining the level of contamination with CD45+ hematopoietic cells using immunohistochemistry and flow cytometry.

Peripheral blood mononuclear cells were isolated from WT and KO mice via density gradient centrifugation using Ficoll-Hypaque (Amersham Pharmacia Biotech, Sweden). CD4+T lymphocytes were further isolated with an immunomagnetic beads method. Cell viability was identified by trypan blue stain assay. The acquired CD4+T-cells were incubated at 37°C in a humidified 5% CO_2 incubator using a complete RPMI 1640 medium (Gibco, Waltham, MA, USA) supplemented with 10% FBS, penicillin and streptomycin (Gibco, Waltham, MA, USA).

T-cell proliferation analysis

The DSS/S1P-induced IECs were used to simulate the *in vivo* condition of IECs. First, the IECs were pretreated with 2% DSS (Sigma-Aldrich, St. Louis, MO, USA) for 12 h, and then they were treated with S1P (Sigma-Aldrich, St. Louis, MO, USA) for 2 h. Prior to the co-culture assays, CD4+T-cells were resuspended in PBS and stained with carboxyfluorescein diacetate succinimidyl ester (CFSE) (Molecular Probes, Eugene, OR, USA). Cells were incubated for 10 min at 37°C with 1 mM CFSE, washed twice with RPMI and used in the co-culture experiments. After that, the IEC was co-cultured with CD4+T-cells in a complete RPMI 1640 medium.

The labeling of T cells with CFSE was performed before the co-cultures. Five days after incubation, T cells were resuspended in PBS and incubated for 30 min with anti-CD3, anti-CD4 and anti-CD8 (conjugated with PE, PerCP or APC, respectively) antibodies and relevant isotype controls (all from Becton Dickinson, Franklin Lakes, NJ, USA). T-cell proliferation was assessed by flow cytometry and four-color analysis of CD3+ lymphocytes using Cell Quest software (Becton Dickinson, Franklin Lakes, NJ, USA). Non-proliferating cells remain high in CFSE expression. In contrast, CFSE expression of proliferating cells decreases in proportion to the number of cell divisions (CFSE-low). After gating on CD3+ cells, percentages of CD4+ cells, CD4− cells, CFSE-high and CFSE-low cells were determined.

Blocking assay

Prior to the co-culture of IEC and CD4+T-cells, IECs were incubated with a purified blocking anti-MHC-II or anti-IFN-γ monoclonal antibody. The cells were then washed twice with PBS and resuspended in medium for co-culture experiments.

RT-qPCR analysis

Total RNA was extracted from the cells using TRIzol reagent according to the manufacturer's instructions. Real-time PCR was conducted using SYBR Premix ExTaq™ (Takara Bio Inc., Shiga, Japan) according to the manufacturer's protocols. For RT-qPCR analysis, all samples were normalized to glyceraldehyde-3-phosphate dehydrogenase (GAPDH). The mean value in each triplicate was used to calculate relative long non-coding RNA (lncRNA) concentrations. Expression fold changes were calculated using $2^{-\Delta\Delta Ct}$ methods.

CT26.WT cell culturing and transfection

Mouse colon carcinoma cell line CT26.WT was purchased from American Type Culture Collection (ATCC) and transfected by a lentivirus of RNA interference for gene S1PR2 (CT26.WT^si-S1PR2 cells), and transfection of control lentivirus was used for the control cells. The cells treated with DSS/IFN-γ were the

Cellular Physiology and Biochemistry

Cell Physiol Biochem 2018;48:1188-1200

DOI: 10.1159/000491985
Published online: July 25, 2018

© 2018 The Author(s). Published by S. Karger AG, Basel
www.karger.com/cpb

1192

Chen et al.: S1P/S1PR2 Pathway in the Intestinal Barrier Function

same as cells treated with DSS/S1P. The CT26.WT$^{si-S1PR2}$ and CT26.WT^{control} cells were treated with DSS/S1P and then co-cultured with CD4$^+$T-cells. The cell supernatant (conditioned medium) of CD4$^+$T-cells and the DSS/S1P-induced CT26.WT^{control} cell or the DSS/S1P-induced CT26.WT$^{si-S1PR2}$ cell co-culture, named control CM and si-S1PR2 CM, respectively, were harvested and preserved.

Trans-epithelial electrical resistance (TER) determination

CT26.WT cells were seeded in a transwell system for monolayers, and then TER values were measured with an epithelial voltohmmeter, ERS-2 (Merck Millipore, Burlington, MA, USA). TER was measured until similar values, calculated with Ω cm^2, were obtained from three consecutive measurements. The TER values of the cells reached at least 500 Ω cm^2 at 20 d, showing the model was successfully established.

Statistical analysis

Data were presented as mean±SD by statistical analysis of ANOVA software combined with t-test. A value of $P < 0.05$ was considered a statistically significant difference.
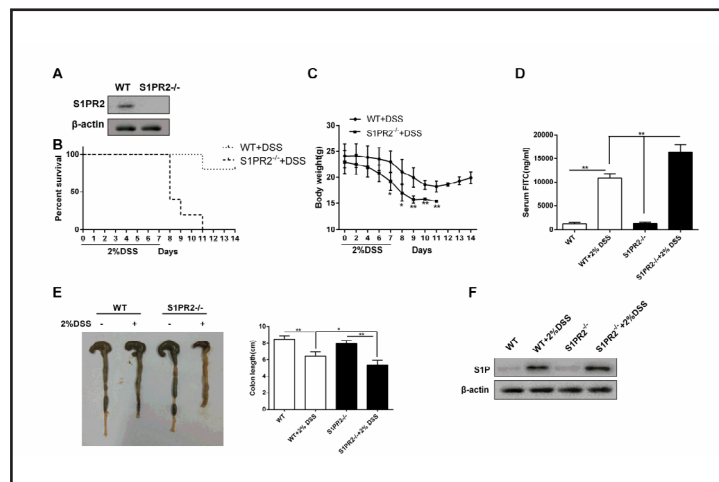
Results

S1PR2$^{-/-}$ mice were susceptible to DSS-induced colitis

To compare the sensitivity to DSS-induced colitis in control and knockout mice (S1PR2$^{-/-}$ mice), we constructed S1PR2$^{-/-}$ mice. The WT and S1PR2$^{-/-}$ mice were treated for 7 d with 2% DSS to induce colitis and then killed at 14 d. 30% body weight reduction can be considered as humane endpoint. Fig. 1A shows the S1PR2 protein expression of colon tissues, which suggests that we were successful in establishing S1PR2$^{-/-}$ mice. After 7 d of treatment with 2% DSS, the survival rates of the WT and S1PR2$^{-/-}$ mice were, respectively, 80% and 40%, indicating a lower survival rate for S1PR2$^{-/-}$ mice after DSS treatment (Fig. 1B). In addition, the body weights of the WT mice were always higher than those of the S1PR2$^{-/-}$ mice, suggesting that the S1PR2$^{-/-}$ mice had more significant weight loss than the WT mice (Fig. 1C).

The mice were divided into four groups (WT, WT+2%, DSS/S1PR2$^{-/-}$/S1PR2$^{-/-}$, and DSS/S1PR2$^{-/-}$/S1PR2$^{-/-}$ +2% DSS). The intestinal permeabilities of the mice are shown by serum FITC concentration in Fig. 1D, which also shows that the DSS-treated mice had higher serum FITC concentrations than the mice not treated with DSS. Moreover, the S1PR2$^{-/-}$ mice had a higher serum FITC concentration than the WT mice, which reveals more serious

Fig. 1. Increased sensitivity to DSS-induced colitis in S1PR2$^{-/-}$ mice. (A) The S1PR2 protein expression of colon tissues in WT and S1PR2$^{-/-}$ mice. (B) Seven days after DSS treatment, the survival rate of WT and S1PR2$^{-/-}$ mice (n=5). (C) The body weight of WT mice was higher than that of S1PR2$^{-/-}$ mice, and S1PR2$^{-/-}$ mice had more significant body weight reduction than WT mice. (D) After DSS treatment, serum FITC concentration was significantly increased in S1PR2$^{-/-}$ mice. **p<0.01, compared with WT or WT+2% DSS or S1PR2$^{-/-}$. (E) S1PR2$^{-/-}$ mice had a shorter colon length than WT mice. *p<0.05, compared with WT+2% DSS. **p<0.01, compared with WT or S1PR2$^{-/-}$. (F) An increased S1P protein expression induced by DSS in both WT and S1PR2$^{-/-}$ mice.

Cellular Physiology and Biochemistry

Cell Physiol Biochem 2018;48:1188-1200

DOI: 10.1159/000491985
Published online: July 25, 2018

© 2018 The Author(s). Published by S. Karger AG, Basel
www.karger.com/cpb

1193

Chen et al.: S1P/S1PR2 Pathway in the Intestinal Barrier Function

intestinal mucosal barrier damage in the S1PR2$^{-/-}$ mice. The total length of colon, shown in Fig. 1E, demonstrates that, after DSS treatment, colon lengths in WT and S1PR2$^{-/-}$ mice were measurably reduced, and the DSS-treated S1PR2$^{-/-}$ mice had shorter colons lengths than the DSS-treated WT mice. Next, we detected the S1P protein expression of colon tissues in the four groups, and the results displayed a weak expression in WT and S1PR2$^{-/-}$ mice and an obviously increased expression in DSS-treated WT and S1PR2$^{-/-}$ mice (Fig. 1F). These data suggest that the S1PR2$^{-/-}$ mice had more sensitivity to DSS-induced colitis than the WT mice.

*The agminated CD4$^+$T-cells in DSS-treated S1PR2$^{-/-}$ mice*

To investigate the colon tissue pathology and CD4$^+$T-cell count at the inflammatory site, the middle section of the mice colons were stained with H&E, and cell suspensions of colonic tissues were prepared. As Fig. 2A shows, the epithelial cells of WT and S1PR2$^{-/-}$ mice maintained integrity, and there were visible goblet cells, with no inflammatory cell infiltration. After DSS treatment, the mucosa of the WT mice was loose, although appearing to be complete, and visible inflammatory cells had infiltrated the intestinal mucosa. The mucosal epithelium of the DSS-treated S1PR2$^{-/-}$ mice had massive quantities of infiltrating inflammatory cells, and the intestinal barrier structure was substantially destroyed, while the goblet cells had disappeared. The H&E stain results clearly demonstrate that DSS induced more serious enteritis in the S1PR2$^{-/-}$ mice.

The obtained mice colon cell suspensions were cultured with RPMI 1640 medium containing 10% FBS for 24 h, and the TNF-α, IL-6 and IFN-γ levels analyzed by ELISA are shown in Figs. 2B, 2C and 2D, respectively. The concentration of IFN-γ, IL-6 and TNF-α produced by the cell suspension had increased in the DSS-induced mice, and the cell suspension from the DSS-induced S1PR2$^{-/-}$ mice had produced higher levels of IFN-γ, IL-6 and TNF-α than the DSS-induced WT mice. Next, the CD4$^+$T-cell and CD4$^+$IFN-γ$^+$ T-cell counts in the cell suspensions were analyzed by flow cytometry; results are shown in Figs. 2E and 2F. The CD4$^+$T-cell counts were increased in the cell suspension from DSS-induced mice, and the cell suspension from the DSS-induced S1PR2$^{-/-}$ mice had higher CD4$^+$T-cell levels and CD4$^+$IFN-γ$^+$ T-cell counts than in the DSS-induced WT mice. These data suggest that in DSS-treated S1PR2$^{-/-}$ mice, there were more CD4$^+$T-cells in the colon tissue.

The IEC promoted CD4$^+$T-cell proliferation by MHC-II

It was previously reported that IECs have the potential to promote CD4$^+$T-cell proliferation [11, 12]. In this study, primary IECs were isolated from four groups (WT group, DSS-induced WT group, S1PR2-deficient group and DSS-treated S1PR2-deficient group), with the isolated IECs named NML WT IEC, IBD WT IEC, NML KO IEC and IBD KO IEC, respectively. These IECs were used as co-cultures with CD4$^+$T-cells to identify their effects on the T-cells. NML WT IEC and NML KO IEC co-cultured with CD4$^+$T-cells both promoted CD4$^+$T-cell proliferation compared to co-culturing with the T cells alone, while there was no significant difference

Fig. 2. The agminated CD4$^+$T-cell in DSS-treated S1PR2$^{-/-}$ mice. (A) The HE staining of the middle section of colon. (B-D) The concentration of IFN-γ, IL-6 and TNF-α produced by the cell suspension from the mouse colon tissue were all increased in cell suspension from the DSS-induced mice with higher levels of IFN-γ, IL-6 and TNF-α in DSS-induced S1PR2$^{-/-}$ mice. (E-F)
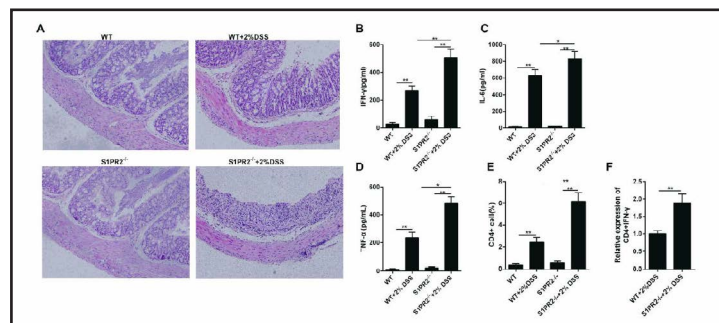
The CD4$^+$T-cell counts were increased in cell suspension from the DSS-induced mice with a higher CD4$^+$T-cell levels and CD4$^+$IFN-γ$^+$ T cell in DSS-induced S1PR2$^{-/-}$ mice. **p<0.01, compared with WT or WT+2% DSS or S1PR2$^{-/-}$.

Chen et al.: S1P/S1PR2 Pathway in the Intestinal Barrier Function

Fig. 3. The IBD intestinal epithelial cells (IEC) promoted CD4+T-cell proliferation and IFN-γ level via increasing MHC-II expression. (A) The IBD KO IEC promoted the proliferation of CD4+T-cell. **p<0.01, compared with WT CD4+T or WT CD4+T +NML IEC or WT CD4+T+IBD IEC. (B) The IBD KO IEC promoted IFN-γ secretion. **p<0.01, compared with WT CD4+T or WT CD4+T +NML IEC or WT CD4+T+IBD IEC. (C)IBD IEC expressed higher surface marker MHC-II than NML IEC, and KO IEC had much higher MHC-II than WT IEC in IBD colons. **p<0.01, compared with NML IEC or IBD IEC. (D) The flow cytometric analysis for MHC-II. (E-F) With the increase of MHC-II antibody (αMHC-II) in the co-culture system, CD4+T-cell proliferation and IFN-γ level were reduced with the increase of αMHC-II c. **p<0.01, compared with no treatment of αMHC-II. Abbreviation: wide type-WT; normal-NML; Inflammatory bowel disease-IBD; Intestinal epithelial cells-IEC.
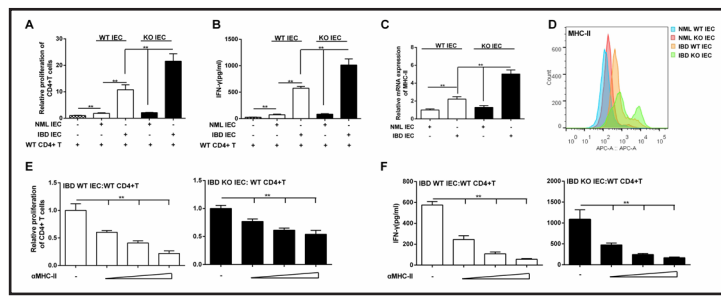
Fig. 4. (A) The S1PR1 and S1PR3 expression were significantly upregulated than other S1P receptors in WT CD4+T-cells. **p<0.01, compared with S1PR2 or S1PR4 or S1PR5. (B)Inhibition of S1PR2 had no significant effect on IFN-γ secretion in CD4+T-cell. (C) Inhibition of S1PR2 had no significant effect on proliferation in CD4+T-cell, and there was no significant differences in proliferation between WT CD4+T and S1PR2−/− CD4+T-cell respectively co-cultured with WT IEC or S1PR2−/− IEC. *p<0.05, compared with CD4+T or S1PR2−/− CD4+. **p<0.01, compared with CD4+T or S1PR2−/− CD4+.
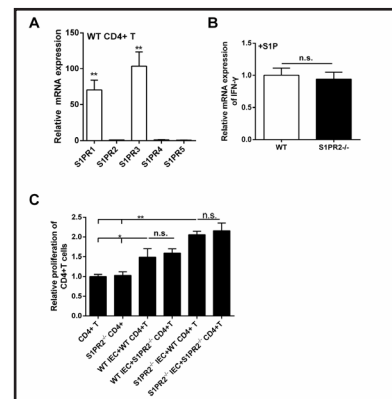

between NML WT IEC and NML KO IEC (Fig. 3A). The IBD IEC in both WT and KO mice appeared to further promote CD4+T-cell proliferation, but the IBD KO IEC was most effective at promoting CD4+T-cell proliferation (Fig. 3A). In the co-cultured system, the IFN-γ secreted by CD4+T-cells had the same trends as with CD4+T-cell proliferation (Fig. 3B).

Former studies have reported that IECs might function as a nonprofessional APC to improve T-cell proliferation [11, 12], and it is known that IECs express the surface antigen presentation molecule MHC-II [13]. Therefore, in order to find the mechanism causing the CD4+T-cell proliferation and IFN-γ production, the MHC-II expressions were tested and were found to have increased more in IBD IECs than in NML IECs. Additionally, KO IECs had greater increases in MHC-II expression than did the WT IECs in IBD mice (Figs. 3C and 3D), which suggests that inhibition of MHC-II could suppress T-cell proliferation in IECs, and S1PR2 might have a certain role in regulating MHC-II expression.

To verify the role of MHC-II in IEC-promoted CD4+T-cell proliferation and IFN-γ levels, MHC-II antibody (αMHC-II) was added into the co-culture system. Both CD4+T-cell proliferation and IFN-γ levels were reduced with increased αMHC-II concentrations (Figs. 3E and 3F), which indicates that the IBD IECs promoted CD4+T-cell proliferation by upregulating MHC-II. For this step, all the CD4+T-cells had been isolated from wild-type mice. As shown in Fig. 4A, the mRNA expressions of S1PR1 and S1PR3 were significantly higher than the S1PR2 expression, which was in a trace amount in the transcription level, suggesting that S1P might play a key role in CD4+T-cells, mainly via S1PR1 and S1PR3, and knockdown of S1PR2 should not significantly affect the CD4+T-cells. Therefore, inhibition of S1PR2 had no measurable effect on either IFN-γ secretion (Fig. 4B) or proliferation of CD4+T-cells (Fig. 4C) in the co-culture system. Hence, the WT CD4+T-cell was chosen for use in this part of the study.

Cellular Physiology and Biochemistry

Cell Physiol Biochem 2018;48:1188-1200

DOI: 10.1159/000491985
Published online: July 25, 2018

© 2018 The Author(s). Published by S. Karger AG, Basel
www.karger.com/cpb

1195

Chen et al.: S1P/S1PR2 Pathway in the Intestinal Barrier Function

To further study whether mouse colon carcinoma cell lines (CT26.WT) could promote CD4$^+$T-cell proliferation by upregulating MHC-II, CT26.WT cells were transfected by a lentivirus of RNA interference for gene S1PR2, with a control lentivirus used for control cells. The S1PR2 protein was not expressed in the CT26.WT$^{si-S1PR2}$ cells, suggesting that the S1PR2 knockout cell line was successfully constructed (Fig. 5A). Surprisingly, MHC-II mRNA expression was almost the same in the DSS-treated si-S1PR2 cells and control cells, and both had a greater increase than the NC group. MHC-II downregulated significantly in the DSS/S1P co-treated group in control cells, while MHC-II remained steady in si-S1PR2 cells after treatment with DSS/S1P compared to treatment with only DSS (Fig. 5A). We had hypothesized that the S1P/S1PR2 axis has the potential to inhibit MHC-II expression. That S1P greatly increased in the mice colons in this study, as shown in Fig. 1F, and was also the upstream signal of S1PR2 could be because the cells lack the S1PR2 upstream stimulate signal molecules, which would explain why CT26.WT$^{si-S1PR2}$ cells showed no significant difference after treatment with DSS compared to the CT26.WT^{control} cells. Hence, we used DSS/S1P co-treatment to modulate the *in vitro* model. CT26.WT cells were treated with DSS/ S1P and co-cultured with CD4$^+$T-cells. The CD4$^+$T-cell proliferation increased significantly more in the co-culture system than in single cultivation, indicating that the DSS/S1P-treated CT26.WT cells could further promote CD4$^+$T-cell proliferation. However, αMHC-II inhibited CD4$^+$T-cell proliferation. In addition, under the DSS/S1P conditions, the CT26.WT$^{si-S1PR2}$ cells were more effective at promoting MHC-II expression than were the CT26.WT^{control} cells (Fig. 5B). The IFN-γ secreted by CD4$^+$T-cells had the same trends as with CD4$^+$T-cell proliferation (Fig. 5C). As compared to single cultivation of CD4$^+$T-cells, the IFN-γ concentration had greatly increased in the co-culture system, indicating that the DSS/S1P treated CT26.WT cells could further promote IFN-γ secretion; however, αMHC-II inhibited IFN-γ secretion. In addition, under the DSS/S1P conditions, the CT26.WT$^{si-S1PR2}$ cells were more effective than

Fig. 5. CT26.WT cell regulated CD4$^+$T-cell proliferation through MHC-II. (A) MHC-II increased its expression in DSS condition, and the addition of S1P partly reversed MHC-
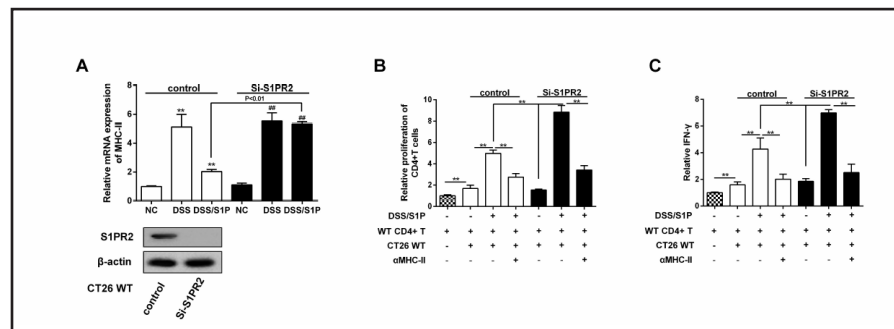
II expression in CT26.WT^{control}, yet no significance change in CT26.WT$^{si-S1PR2}$, which resulted in a much higher expression in CT26.WT$^{si-S1PR2}$ after co-treatment with DSS/S1P than that in CT26.WT^{control} **p<0.01, compared with NC. (B) The CD4$^+$T-cell proliferation were increased highly in co-culture system than single cultivation. The CT26.WT cell treated with DSS/S1P could further promote CD4$^+$T-cell proliferation, but αMHC-II inhibited CD4$^+$T-cell proliferation, which partly reversed the role of DSS/S1P-treated CT26.WT cell. In addition, under the DSS/S1P conditions, the CT26.WT$^{si-S1PR2}$ cell was more effective than CT26.WT^{control} cell in promoting MHC-II expression. **p<0.01, compared with WT CD4$^+$T or WT CD4$^+$T+CT26 WT or WT CD4$^+$T+CT26.WT+DSS/S1P or WT CD4$^+$T+CT26.WT+DSS/S1P+αMHC-II. (C) Comparing to single cultivation of CD4$^+$T-cell, the IFN-γ concentration was increased highly in co-culture system. The CT26.WT cell treated with DSS/S1P could further promote IFN-γ secretion, but αMHC-II inhibited IFN-γ secretion, which partly reversed the role of DSS/S1P-treated CT26.WT cell. In addition, under the DSS/S1P conditions, the CT26. WT$^{si-S1PR2}$ cell was more effective than CT26.WT^{control} cell in promoting IFN-γ secretion. **p<0.01, compared with WT CD4$^+$T or WT CD4$^+$T+CT26.WT or WT CD4$^+$T+CT26.WT+DSS/S1P or WT CD4$^+$T+CT26.WT+DSS/ S1P+αMHC-II.

Cellular Physiology and Biochemistry

Cell Physiol Biochem 2018;48:1188-1200

DOI: 10.1159/000491985
Published online: July 25, 2018

© 2018 The Author(s). Published by S. Karger AG, Basel
www.karger.com/cpb

1196

Chen et al.: S1P/S1PR2 Pathway in the Intestinal Barrier Function

the CT26[control] cells in promoting IFN-γ secretion. These data demonstrate that IECs promoted CD4^{+}T-cell proliferation by upregulating MHC-II.

S1P/S1PR2 controlled MHC-II expression to regulate CD4^{+}T-cell proliferation via ERK

To explore whether the ERK signaling pathway is involved in S1P/S1PR2-controlled MHC-II expression to regulate CD4^{+}T-cell proliferation, the antagonist of S1PR2 (JTE-013) and ERK inhibitor (U0126) were used to inhibit S1PR2 expression and prevent ERK phosphorylation, respectively. As shown in Figs. 6A and 6B, the S1PR2 mRNA expressions were significantly greater than those of other S1P receptors in IEC and CT26.WT cells, which revealed that S1P played a key role in these cells, mainly via S1PR2. In the S1P environment, p-ERK expression was reduced in KO IECs and CT26.WT[si-S1PR2] cells, suggesting that reduced S1PR2 expression inhibited p-ERK expression (Fig. 6C). Compared with the control CT26.WT cells, the DSS or DSS/S1P-treated CT26.WT cells had more MHC-II expression. In addition, the JTE-013 and U0126 further upregulated MHC-II expression, which indicates that S1P/S1PR2 regulated MHC-II expression through ERK (Figs. 6D and 6E). The CT26.WT[si-S1PR2] cells and CT26.WT[control] cells were co-cultured with CD4^{+}T-cells. U0126 promoted CD4^{+}T-cell proliferation and IFN-γ secretion, especially in the CT26.WT[si-S1PR2] cell co-cultured system (Fig. 6F). These data suggest that S1P/S1PR2 controlled MHC-II expression to regulate CD4^{+}T-cell proliferation via ERK.

Mechanisms of S1PR2^{−/−} mice suffering more severe intestinal barrier injuries

The CD4^{+}T-cell-secreted IFN-γ increased DSS-induced damage of intestinal epithelial cell barrier function, and to investigate this damage, CT26.WT cells were seeded in a transwell system for monolayers to construct an intestinal epithelial barrier model. The TER values of the cells reached at least 500 Ω cm^2 at 20 d, demonstrating that the model was successfully established. It was shown that the CD4^{+}T-cells in S1PR2^{−/−} mice and those in the si-S1PR2 co-culture system produced more IFN-γ. IFN-γ plays an indispensable role in the initiation of DSS colitis [14], and we tried to evaluate whether increased levels of IFN-γ would accelerate the intestinal barrier disruption. To that end, we built a Caco-2 monolayer to simulate the intestinal barrier *in vivo*. First, the TER values of the Caco-2[si-S1PR2] cells and CT26.WT[control] cells both reached at least 500 Ω cm^2 at 20 d, showing a successfully established intestinal

Fig. 6. S1P/S1PR2 controlled MHC-II expression to regulate CD4^{+}T-cell proliferation via ERK (A-B) The mRNA expression of S1P receptors 1–5 (S1PR1–5) were detected in IEC and CT26.WT cell. S1PR2 expression was significantly higher than other S1P receptors. **p<0.01, compared with S1PR2. (C) In S1P environment, the p-ERK expression was reduced in KO IEC and CT26.WT[si-S1PR2] cell. (D) Blockingf ERK (U0126) or S1PR2 (JTE-013) signal in CT26.WT cell increased MHC-II expression. **p<0.01, compared with DSS or DSS+S1P or DSS+S1P+U0126. (E) The flow cytometric analysis for MHC-II. (F and G) The CT26.WT[si-S1PR2] cell and CT26.WT[control] cell were co-cultured with CD4^{+}T-cell, respectively. Inhibition of ERK (U0126) or S1PR2 in CT26.WT cell promoted CD4^{+}T-cell proliferation and IFN-γ secretion. **p<0.01, compared with DSS/S1P or DSS/S1P+U0126.
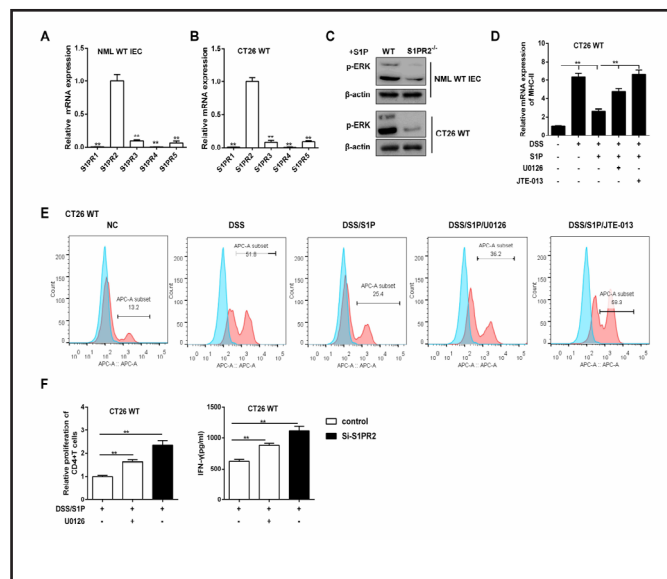
1197

Chen et al.: S1P/S1PR2 Pathway in the Intestinal Barrier Function

Fig. 7. IFN-γ from CD4^{+}T-cells enhanced DSS-induced damage of intestinal epithelial cell barrier function and S1P/S1PR2 partly reduced this injury. (A) The TER values of the Caco-2[si-S1PR2] cell and Caco-2[control] cells both reached at least 500 Ω cm^2 at 20 d. (B) The increasing IFN-γ enhanced the DSS induced damage in TER in Caco-2[control] and Caco-2[si-S1PR2]. **$p<0.01$, compared with control. #$p<0.05$, compared with 2% DSS. ##$p<0.01$, compared with 2% DSS. (C) The increasing IFN-γ enhanced the DSS induced damage in intestinal permeability both in Caco-2[control] and Caco-2[si-S1PR2]. **$p<0.01$, compared with control. #$p<0.05$, compared with 2% DSS. ##$p<0.01$, compared with 2% DSS. (D) S1P/S1PR2 axis efficiently reduced the intestinal barrier damage induced by DSS in Caco-2[control] monolayer. **$p<0.01$, compared with control or DSS/IFN-γ or DSS/IFN-γ+S1P (E) S1P promoted ZO-1 expression, and blocking S1P/S1PR2 signals blocked ZO-1 expression. (F-G) In Caco-2[s-S1PR2] cell, DSS/IFN-γ obviously inhibited TER value. **$p<0.01$, compared with control.
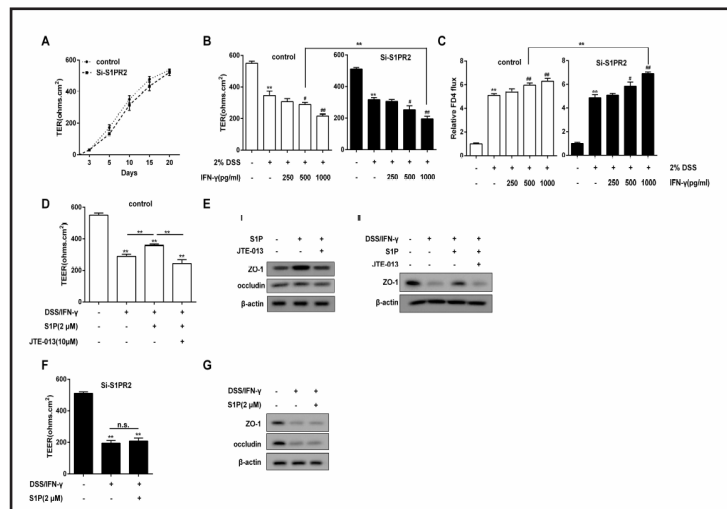
epithelial barrier model (Fig. 7A). In addition, in CT26.WT cells treated with DSS, as increased levels of IFN-γ appeared, TER gradually lowered, and FD4 values increased in Caco-2[control] and Caco-2[si-S1PR2] (Figs. 7B and 7C). Further, under the DSS cultured medium, the addition of IFN-γ promoted barrier disruption, and there is a close correlation between the IFN-γ and TER or FD4 values in the Caco-2[control] group ($r = -0.994$ and $P = 0.006$ with TER, while $r = 0.968$ and $P = 0.032$ with FD4) and in the Caco-2[si-S1PR2] group ($r = -0.984$ and $P = 0.016$ with TER, while $r = 0.990$ and $P = 0.010$ with FD4).

It could, therefore, be speculated that S1PR2-deficient mice suffered severe intestinal barrier injury partly due to the greater quantities of IFN-γ that the CD4^{+}T-cells secreted.

Mechanisms of S1P mice suffering less severe intestinal barrier injury

As opposed to the above, S1P suppressed DSS/IFN-γ-damaged permeability of intestinal mucosa. The DSS/IFN-γ treatment was used to simulate the enteritis microenvironment *in vivo*, and after adding S1P to the conditioned medium, the intestinal barrier disruption induced by DSS was partly reversed (Fig. 7D). In Caco-2 cells, S1P/S1PR2 promoted ZO-1 expression, and through the S1PR2 special antagonist JTE-013, we can conclude that the S1P/S1PR2 axis regulates the intestinal barrier and promotes ZO-1 expression (Fig. 7E). However, S1P could not reverse the downregulated ZO-1 expression and reduce the intestinal barrier permeability induced by the DSS/IFN-γ in Caco-2[si-S1PR2] cells (Figs. 7F and 7G) because S1P/S1PR2 couldn't function there. These data imply that S1P could reduce the DSS/IFN-γ damaged permeability of the intestinal mucosa, and it might be associated with increased ZO-1 in Caco-2 cells. Therefore, we thought that S1P/S1PR2 could efficiently function on ZO-1, and the intestinal barrier permeability in S1PR2$^{-/-}$ might be another mechanism to illustrate that S1PR2$^{-/-}$ mice suffered more severe intestinal barrier injury.

Discussion

Acute DSS-induced colitis in mice is frequently used as an *in vivo* model for analysis of intestinal mucosal barrier damage implicated in human pathophysiology. The S1PR2

KARGER

Cellular Physiology and Biochemistry

Cell Physiol Biochem 2018;48:1188-1200

DOI: 10.1159/000491985
Published online: July 25, 2018

© 2018 The Author(s). Published by S. Karger AG, Basel
www.karger.com/cpb

1198

Chen et al.: S1P/S1PR2 Pathway in the Intestinal Barrier Function

protein expression of colon tissues in S1PR2$^{-/-}$ mice suggested that we were successful in establishing S1PR2$^{-/-}$ mice in this study. After DSS treatment, the survival rate of S1PR2$^{-/-}$ mice was significantly lower than that of the WT mice, and the S1PR2$^{-/-}$ mice had more severe intestinal mucosal barrier damage and shorter colon lengths. Moreover, H&E staining of the middle section of the colons showed that the mucosal epithelium of DSS-induced S1PR2$^{-/-}$ mice had been significantly infiltrated with inflammatory cells, and the normal epithelial cells and goblet cells were not seen. These results strongly suggest an increased sensitivity and more serious DSS-induced colitis in the S1PR2$^{-/-}$ mice than in the WT mice. We investigated the concentration of pro-inflammatory cytokines, such as IFN-γ, IL-6 and TNF-α, as well as the cell counts of CD4$^+$T-cells and CD4$^+$ IFN-γ$^+$ T cells, in isolated cell suspension from the mouse colon tissue. Considerable research has shown that DSS-induced acute colitis is correlated with increased production of IFN-γ, IL-6 and TNF-α[15, 16], along with CD4$^+$T-cell accumulation and infiltration in the colonic *lamina propria* [17, 18]. In this study, we found that after DSS treatment, S1PR2$^{-/-}$ mice produced higher levels of IFN-γ, IL-6 and TNF-α and also had higher cell counts of CD4$^+$T-cells and CD4$^+$ IFN-γ$^+$ T cells than WT mice, which implies that the importance of the role of the S1P/S1PR2 axis in DSS-induced colitis is associated with CD4$^+$T-cell activation.

To further investigate the effect of IECs on CD4$^+$T-cells in mucosal homeostasis and intestinal inflammation, the isolated IECs from WT and S1PR2$^{-/-}$ mice were co-cultured with CD4$^+$T-cells isolated from WT mice and treated with DSS/S1P. This *in vitro* model allowed us to focus on the differences in proliferation and IFN-γ secretion of CD4$^+$T-cells induced by KO IECs that were isolated from S1PR2$^{-/-}$ mice, and the WT IECs isolated from WT mice were less effective than the KO IECs. Dotan et al [6]. reported that co-cultures of normal CD4$^+$T-cells and IECs derived from IBD patients resulted in a preferential activation of CD4$^+$T-cell proliferation that was associated with significant IFN-γ. MHC class II molecules are a family of molecules normally found only on antigen-presenting cells such as mast cells, dendritic cells, mononuclear phagocytes, some endothelial cells, thymic epithelial cells, and B cells, and research has demonstrated the capacity of these cells for presenting antigens by class II MHC molecules to CD4$^+$T-cells [19-21]. Our results showed for the first time that the KO IEC was more effective in promoting the proliferation and IFN-γ secretion of CD4$^+$T-cells, and in the co-culture system with a DSS/S1P environment, the CD4$^+$T-cell proliferation and IFN-γ levels were both reduced with the increase of αMHC-II concentrations. Thus, we concluded that the S1PR2$^{-/-}$ IECs were more effective in promoting the proliferation of IFN-γ and secretion of CD4$^+$T-cells, which was relevant to the increased MHC-II expression in KO IECs. We used the CT26.WT mouse colon carcinoma cell line to verify the effects of S1PR2 IECs on the proliferation of IFN-γ and secretion of CD4$^+$T-cells. The CT26.WT cells were transfected by a lentivirus of RNA interference for gene S1PR2, treated with DSS/S1P and co-cultured with CD4$^+$T-cells. The MHC-II expression was increased in CT26.WT$^{si-S1PR2}$ cells, which were more effective than CT26.WT^{control} cells in promoting CD4$^+$T-cell proliferation and IFN-γ secretion, suggesting the role of the S1P/S1PR2 axis in IEC-mediated CD4$^+$T-cell activation via MHC-II expression.

The intestinal DC in irritable bowel syndrome rats showed an upregulated expression of MHC-II, which may be related to the activation of the intracellular ERK1/2 pathway [22]. Previous studies have reported that S1P protected liver injury which might activate hepatic stellate cells [23, 24]. Importantly, S1P protected IECs from apoptosis by activating the ERK and Akt signaling pathways [4]. Next, we examined whether the S1P/S1PR2 axis controlled MHC-II expression to regulate CD4$^+$T-cell activation via ERK signaling. In our study, the p-ERK expressions were reduced in KO IECs and CT26.WT$^{si-S1PR2}$ cells, and inhibition of ERK (U0126) or SIPR2 (JTE-013) in CT26.WT cells increased MHC-II expression. When the MHC-II expression is co-cultured with CD4$^+$T-cells, it may function to promote CD4$^+$T-cell proliferation and IFN-γ secretion, proving that S1P/S1PR2 controlled MHC-II expression through ERK to regulate CD4$^+$T-cell activation.

IFN-γ plays an important role in intestinal barrier dysfunction. A study by Yang et al [25]. reported that IFN-γ induced the loss of epithelial barrier function and disruption of tight

Cellular Physiology and Biochemistry

Cell Physiol Biochem 2018;48:1188-1200

DOI: 10.1159/000491985
Published online: July 25, 2018

© 2018 The Author(s). Published by S. Karger AG, Basel
www.karger.com/cpb

1199

Chen et al.: S1P/S1PR2 Pathway in the Intestinal Barrier Function

junction proteins (ZO-1 and claudin-1) by upregulating HIF-1α through the NF-κB pathway. The combination of IFN-γ and TNF-α can induce intestinal epithelial barrier dysfunction by upregulating myosin light chain kinase (MLCK) protein expression and promoting MLCK protein phosphorylation [26]. Our study using the harvested cell co-conditioned medium of CD4^{+}T-cells and si-S1PR2 CM cells or control CM cells constructed an intestinal epithelial barrier model to simulate an *in vivo* microenvironment. Not surprisingly, compared to the control CM, adding si-S1PR2 CM decreased the TER value and increased intestinal permeability, which created more severe effects when the IFN-γ antibody is involved. Thus, the CD4^{+}T-cell-secreted IFN-γ increased DSS-induced damage of the intestinal epithelial cell barrier function. In addition, we found that IFN-γ induced the loss of epithelial barrier function by downregulating ZO-1, while S1P could suppress DSS/IFN-γ-damaged permeability of intestinal mucosa by increasing ZO-1.

In conclusion, our study found that enteritis epithelial cells promoted CD4^{+}T-cell proliferation, and further, the IFN-γ secreted from CD4^{+}T-cells further aggravated the damage to the intestinal barrier function of the enteritis. However, S1P and its receptor, S1PR2, partly relieved the damage through enhancing ZO-1 expression, and inhibition of S1PR2 rendered the S1P useless in protecting intestinal mucosa. Thus, there was more serious intestinal mucosal barrier damage in S1PR2^{-/-} mice.

Acknowledgements

Disclosure Statement

The authors declare to have no competing interests.

References

1   Greenspon J, Li R, Xiao L, Rao JN, Marasa BS, Strauch ED, Wang JY, Turner DJ: Sphingosine-1-phosphate protects intestinal epithelial cells from apoptosis through the akt signaling pathway. Digest Diseas Sci 2009;54:499.

2   Jiang P, Smith AD, Li R, Rao JN, Liu L, Donahue JM, Wang JY, Turner DJ: Sphingosine kinase 1 overexpression stimulates intestinal epithelial cell proliferation through increased c-myc translation. Am J Physiol Cell Physiol 2013;304:C1187.

3   Zhang G, Yang L, Kim GS, Ryan K, Lu S, O'Donnell RK, Spokes K, Shapiro N, Aird WC, Kluk MJ: Critical role of sphingosine-1-phosphate receptor 2 (s1pr2) in acute vascular inflammation. Blood 2013;122:443.

4   Chen T, Huang Z, Liu R, Yang J, Hylemon PB, Zhou H: Sphingosine-1 phosphate promotes intestinal epithelial cell proliferation via s1pr2. Front Biosci 2017;22:596.

5   Chen T, Xue H, Lin R, Huang Z: Mir-126 impairs the intestinal barrier function via inhibiting s1pr2 mediated activation of pi3k/akt signaling pathway. Biochem Biophys Res Commun 2017;494:427-432.

6   Dotan I, Allez M, Nakazawa A, Brimnes J, Schulder-Katz M, Mayer L: Intestinal epithelial cells from inflammatory bowel disease patients preferentially stimulate cd4+ t cells to proliferate and secrete interferon-gamma. Am J Physiol Gastrointest Liver Physiol 2007;292:1630-1640.

7   Oskeritzian CA, Hait NC, Wedman P, Chumanevich A, Kolawole EM, Price MM, Falanga YT, Harikumar KB, Ryan JJ, Milstien S: The s1p/s1pr2 axis regulates early airway t cell infiltration in murine mast cell-dependent acute allergic responses. J Allergy Clin Immunol 2015;135:1008-1018.

8   Ishii I, Ye X, Friedman B, Kawamura S, Contos JJA, Kingsbury MA, Yang AH, Zhang G, Brown JH, Chun J: Marked perinatal lethality and cellular signaling deficits in mice null for the two sphingosine 1-phosphate (s1p) receptors, s1p2/lpb2/edg-5 and s1p3/lpb3/edg-3. J Biol Chem 2002;277:25152.

Cellular Physiology and Biochemistry

Cell Physiol Biochem 2018;48:1188-1200

DOI: 10.1159/000491985
Published online: July 25, 2018

© 2018 The Author(s). Published by S. Karger AG, Basel
www.karger.com/cpb

1200

Chen et al.: S1P/S1PR2 Pathway in the Intestinal Barrier Function

9   Ishii I, Friedman B, Ye X, Kawamura S, Mcgiffert C, Contos JJ, Kingsbury MA, Zhang G, Brown JH, Chun J: Selective loss of sphingosine 1-phosphate signaling with no obvious phenotypic abnormality in mice lacking its g protein-coupled receptor, lp(b3)/edg-3   J Biol Chem 2001;276:33697-33704.

10   Ma Y, Yue J, Zhang Y, Shi C, Odenwald M, Liang WG, Wei Q, Goel A, Gou X, Zhang J: Acf7 regulates inflammatory colitis and intestinal wound response by orchestrating tight junction dynamics. Nat Commun 2017;8:15375.

11   Dahan S, Rabinowitz KM, Martin AP, Berin MC, Unkeless JC, Mayer L: Notch-1 signaling regulates intestinal epithelial barrier function, through interaction with cd4+ t cells, in mice and humans. Gastroenterology 2011;140:550-559.

12   Olivares-Villagómez D, Algood H, Singh K, Parekh V, Ryan K, Piazuelo M, Wilson K, Van Kaer L: Intestinal epithelial cells modulate cd4 t cell responses via the thymus leukemia antigen. J Immunol 2011;187:4051-4060.

13   Büning J, Von SD, Tafazzoli K, Zimmer KP, Strobel S, Apostolaki M, Kollias G, Heath JK, Ludwig D, Gebert A: Multivesicular bodies in intestinal epithelial cells: Responsible for mhc class ii-restricted antigen processing and origin of exosomes. Immunology 2008;125:510.

14   Deguchi Y, Andoh A, Yagi Y, Bamba S, Inatomi O, Tsujikawa T, Fujiyama Y: The s1p receptor modulator fty720 prevents the development of experimental colitis in mice. Oncol Rep R 2006;16:699.

15   Azuma YT, Nishiyama K, Matsuo Y, Kuwamura M, Morioka A, Nakajima H, Takeuchi T: Pparα contributes to colonic protection in mice with dss-induced colitis. Int Immunopharmacol 2010;10:1261-1267.

16   Xiao YT, Yan WH, Cao Y, Yan JK, Cai W: Neutralization of il-6 and tnf-α ameliorates intestinal permeability in dss-induced colitis. Cytokine 2016;83:189-192.

17   Radulovic K, Rossini V, Manta C, Holzmann K, Kestler HA, Niess JH: The early activation marker cd69 regulates the expression of chemokines and cd4 t cell accumulation in intestine. Plos One 2013;8:e65413.

18   Suwandi A, Bargen I, Pils MC, Krey M, Lage SZ, Singh AK, Basler T, Falk CS, Seidler U, Hornef MW: Cd4 t cell dependent colitis exacerbation following re-exposure of mycobacterium avium ssp. Paratuberculosis. Front Cell Infect Microbiol 2017;7:75.

19   Elieh DAK, Grauwet K: Role of mast cells in regulation of t cell responses in experimental and clinical settings. Clin Rev Allergy Immunol 2017:1-14.

20   Rocha-Perugini V, Martínez DHG, González-Granado JM, Ramírez-Huesca M, Zorita V, Rubinstein E, Boucheix C, Sánchez-Madrid F: Cd9 regulates mhc-ii trafficking in monocyte-derived dendritic cells. Mol Cell Biol 2017;37.

21   Rouhani SJ, Eccles JD, Riccardi P, Peske JD, Tewalt EF, Cohen JN, Liblau R, Mäkinen T, Engelhard VH: Roles of lymphatic endothelial cells expressing peripheral tissue antigens in cd4 t-cell tolerance induction. Nat Commun 2015;6:6771.

22   Li M, Hu Y, Wang X, Lu B, Zhang M, Chen C: Effect of erk1/2 pathway in the expression of mhc-of intestinal dendritic cells in viscerally hypersensitive rats. Zhonghua yi xue za zhi 2015;95:3930-3934.

23   Al FF, Fayyaz S, Japtok L, Kleuser B: Involvement of sphingosine 1-phosphate in palmitate-induced non-alcoholic fatty liver disease. Cell Physiol Biochem 2016;40:1637.

24   Du Y, Li D, Han C, Wu H, Xu L, Zhang M, Zhang J, Chen X: Exosomes from human-induced pluripotent stem cell–derived mesenchymal stromal cells (hipsc-mscs) protect liver against hepatic ischemia/ reperfusion injury via activating sphingosine kinase and sphingosine-1-phosphate signaling pathway. Cell Physiol Biochem2017;43:611-625.

25   Yang S, Yu M, Sun L, Xiao W, Yang X, Sun L, Zhang C, Ma Y, Yang H, Liu Y, Lu D, Teitelbaum DH, Yang H: Interferon-γ-induced intestinal epithelial barrier dysfunction by nf-κb/hif-1α pathway. J Interferon Cytokine Res 2014;34:195-203.

26   Liu H, Wang P, Wang FJ: An experimental study on intestinal epithelial barrier dysfunction induced by interferon-gamma and tumor necrosis factor-alpha. Zhonghua shao shang za zhi 2011;27:145.